AGU PUBLICATIONS

Geophysical Research Letters

RESEARCH LETTER

10.1002/2016GL068727

Key Points:
- Gas transfer velocities are measured with the $^3He/SF_6$ technique in a mangrove estuary for the first time
- A gas exchange parameterization that takes into account current velocity and wind speeds is proposed
- Water residence times are determined from SF_6 inventory, after correcting for gas exchange

Supporting Information:
- Supporting Information S1
- Data Set S1

Correspondence to:
D. T. Ho,
ho@hawaii.edu

Citation:
Ho, D. T., N. Coffineau, B. Hickman, N. Chow, T. Koffman, and P. Schlosser (2016), Influence of current velocity and wind speed on air-water gas exchange in a mangrove estuary, *Geophys. Res. Lett.*, *43*, doi:10.1002/2016GL068727.

Received 17 MAR 2016
Accepted 26 MAR 2016
Accepted article online 31 MAR 2016

Influence of current velocity and wind speed on air-water gas exchange in a mangrove estuary

David T. Ho[1], Nathalie Coffineau[1], Benjamin Hickman[1], Nicholas Chow[1], Tobias Koffman[2], and Peter Schlosser[2]

[1]Department of Oceanography, University of Hawai'i at Mānoa, Honolulu, Hawaii, USA, [2]Lamont-Doherty Earth Observatory, Columbia University, Palisades, New York, USA

Abstract Knowledge of air-water gas transfer velocities and water residence times is necessary to study the fate of mangrove derived carbon exported into surrounding estuaries and ultimately to determine carbon balances in mangrove ecosystems. For the first time, the $^3He/SF_6$ dual tracer technique, which has been proven to be a powerful tool to determine gas transfer velocities in the ocean, is applied to Shark River, an estuary situated in the largest contiguous mangrove forest in North America. The mean gas transfer velocity was 3.3 ± 0.2 cm h^{-1} during the experiment, with a water residence time of 16.5 ± 2.0 days. We propose a gas exchange parameterization that takes into account the major sources of turbulence in the estuary (i.e., bottom generated shear and wind stress).

1. Introduction

Mangrove ecosystems are critical transition zones between the land and ocean in tropical and subtropical areas [*Levin et al.*, 2001]. They offer many ecosystem services, including coastal protection and nursery habitat, and are among the most productive ecosystems on the planet [*Bouillon et al.*, 2008]. However, to determine the fate of carbon sequestered by mangroves and to understand the role of these ecosystems in regional and global carbon cycle requires knowledge about air-water CO_2 fluxes and longitudinal export of carbon to the coastal ocean. Quantification of fluxes by these pathways depends on information about the rate of air-water gas exchange and residence time of water in the mangrove estuary. Furthermore, in these settings, the use of ^{222}Rn to quantify groundwater discharge or tidal flushing of crab burrows also requires knowledge of the gas transfer velocity [*Maher et al.*, 2013; *Stieglitz et al.*, 2013].

Our ability to parameterize gas exchange between the atmosphere and the open ocean has improved dramatically in the last couple of decades, in part because of advances in techniques designed to study gas exchange on time scales of hours to days. However, as we move toward coastal areas and inland waters, the ability of existing parameterizations between environmental variables and gas exchange to accurately predict the gas transfer velocities decreases, owing to increase uncertainty in factors contributing to generation of near-surface turbulence. This is probably due to the fact that as water depths shoal, other factors such as bottom roughness and currents can generate turbulence and enhance gas exchange.

Knowledge of water residence time is important for determining carbon balance, because the amount of time water spends in the estuary determines how much time it has to receive inputs from mangrove, how much time there is for organic carbon to transform to inorganic carbon via pathways such as respiration or photodegredation, and how much time dissolved CO_2 and CH_4 in water has to exchange with the atmosphere.

The $^3He/SF_6$ technique has emerged as one of the most robust methods for determining gas transfer velocities on times scales of days to weeks in the ocean [*Watson et al.*, 1991; *Wanninkhof et al.*, 1993] and has allowed the uncertainty in the relationship between wind speed and gas exchange to be narrowed [*Ho et al.*, 2011b]. In addition, the inventory of SF_6, corrected for gas exchange, yields information about water residence time.

The $^3He/SF_6$ technique has previously been applied in the Hudson River, a large tidal estuary in the northeastern United States [*Clark et al.*, 1994, 1995; *Ho et al.*, 2011a]. Here, for the first time, the technique is applied in a mangrove estuary to determine gas transfer velocities and to derive a relationship that

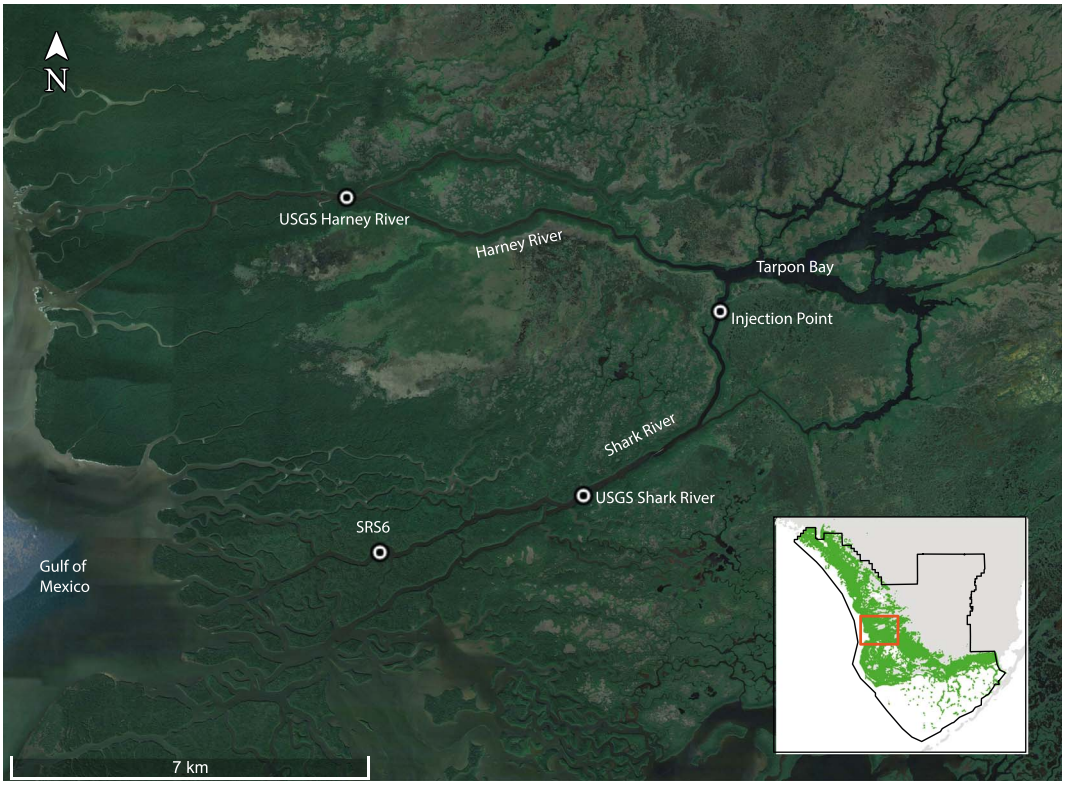

Figure 1. Satellite image showing the study area, including Shark River, Harney River, Tarpon Bay, and the Gulf of Mexico. The locations of the SRS6 CO_2 eddy flux tower, as well as the two USGS gaging stations, are also indicated. The inset shows the boundaries of Everglades National Park and the boundary of the satellite image. In green is the extent of the mangrove forest.

combines the effect of current velocity and wind speed on gas exchange. Furthermore, the SF_6 inventory is used to determine water residence time and to evaluate the freshwater fraction model of estuary water residence time.

2. Methods

2.1. Study Site

This study was conducted in Shark River (Figure 1), a tidal estuary situated wholly within the western part of Everglades National Park in Southern Florida, USA, and flows through the largest contiguous mangrove forest in North America. This subtropical region has a distinct wet and dry season, with the wet season beginning in May and lasting until October. Climatologically, 76% of the precipitation falls during the wet season.

Shark River begins at Tarpon Bay, and flows for approximately 15 km into the Gulf of Mexico. The river is fringed by three species of mangroves, *Laguncularia racemosa, Avicennia germinans, and Rhizophora mangle*.

2.2. Shark River Tracer Release Experiment

Shark River Tracer Release Experiment (SharkTREx) is a series of studies conducted in Shark River to examine air-water gas exchange, longitudinal dispersion, and residence time of water in the estuary and to provide a Lagrangian framework for examining input and transformation of organic and inorganic carbon into the river. SharkTREx 1 and 2 were conducted from 19 to 25 November 2010 and 9 to 15 November 2011, respectively, and have been described in *Ho et al.* [2014]. This experiment described here, conducted from 25 to 31 October 2014, is the third in the series and will be referred to as SharkTREx 3.

During SharkTREx 3, a houseboat was used to conduct underway surveys of SF_6, temperature, and salinity and to provide a platform from which discrete samples for ^3He and SF_6 were taken. The details of the measurements are given below. The experiment also involved the use of other smaller boats and extensive

measurements of organic and inorganic carbon parameters (including carbon isotopes), water isotopes, and radioisotopes as indicators for groundwater input to determine the sources of sinks of carbon in this ecosystem; the results of which will be presented elsewhere.

2.3. Wind Speeds and Current Velocities

During SharkTREx 3, wind speeds were only measured from the houseboat during the day and from a small boat on certain days during specific operations. The 3-D ultrasonic anemometer at the CO_2 eddy flux tower (SRS6; 25.3646, −81.0779; Figure 1) in the mangrove forest bordering Shark River was not fully functional during the study period. For consistency and completeness, the analysis here uses wind speeds measured by a 2-D ultrasonic anemometer mounted at 10 m height at a nearby land-based station (Homestead; 25.5126, −80.5031) scaled by an appropriate factor (see below). The wind speeds at this station were sampled every 5 s and averaged every 15 min.

An extensive comparison of 4 years of data from Homestead and SRS6 (nearly 65,000 measurements) shows that the wind speeds measured at SRS6 can be approximated by a linear scaling of the measurement at Homestead (lower by a factor of 1.729). The reconstructed data from Homestead has the same pattern and the same mean and standard deviation as the SRS6 data over the same time interval. Furthermore, the scaled Homestead wind speed data are in good general agreement with the limited wind speeds measured at the SRS6 CO_2 eddy flux tower during SharkTREx 3 (see Figure 2b) and in good agreement with wind speed measured at a station in the middle of the river during SharkTREx 2 in 2011 (see supporting information).

Current velocities were measured by the U.S. Geological Survey at a station (USGS 252230081021300 Shark River below Gunboat Island; Figure 1) near the midpoint of Shark River. The measurements were available every 15 min for most of the experiment. For periods when current velocity data were missing, the relationship between data from a nearby station (USGS 252551081050900 Harney River; Figure 1) and the Shark River station was used to reconstruct the Shark River data. The reconstructed data for Shark River for the entire period are in good agreement with the measured data (see Figure 2a).

2.4. Tracer Injection

^{3}He and SF_6 were injected into the river approximately 0.7 km downstream of Tarpon Bay (Figure 1) on 24 October 2014. A mixture from a compressed gas cylinder, containing ^{3}He and SF_6 at a ratio of 1 to 340, was bubbled through a length of diffusion tubing into the water near the bottom (2 to 2.5 m depth) from a small boat as it traversed the width of the river over a period of 5 min.

2.5. Underway SF_6, Salinity, and Temperature

For seven consecutive days after injection (25–31 October 2014), underway measurements were made for water temperature, salinity, and SF_6 from an intake at the front of the houseboat, from about 0.5 m depth, as the boat traversed down the center of the river from Tarpon Bay out to the Gulf of Mexico and back. The temperature and salinity measurements were made at a frequency of 1 Hz with a thermosalinograph (Sea-Bird SBE 45 MicroTSG) situated near the water intake to minimize heating, and the SF_6 was measured with an automated analysis system described in detail in *Ho et al.* [2002]. The system provides a near real-time measurement of the SF_6 in the surface water with a time resolution of approximately 1 min and allowed the discrete sampling of ^{3}He and SF_6 to be conducted near the peak of the tracer patch.

2.6. Discrete ^{3}He and SF_6

During SharkTREx 3, water samples were taken with a 5 L Niskin bottle at a depth of 1.1 m. Simultaneous profiles of temperature and salinity were made with a conductivity, temperature, and depth sonde (SonTek CastAway-CTD) and used to determine physicochemical properties of the tracers. From depth profiles of temperature and salinity taken during SharkTREx 3, along with temperature, salinity, dissolved oxygen, and SF_6 taken during SharkTREx 1 and 2 [*Ho et al.*, 2014], it was determined that because of its relatively shallow depth and vigorous mixing from tides, the river is well mixed, and a single sample is representative of the water column.

Samples for SF_6 (10 to 40 ml, depending on the expected SF_6 concentrations) were taken in 50 mL glass syringes and stored under water in a cooler until analysis back at the shore-based laboratory in the

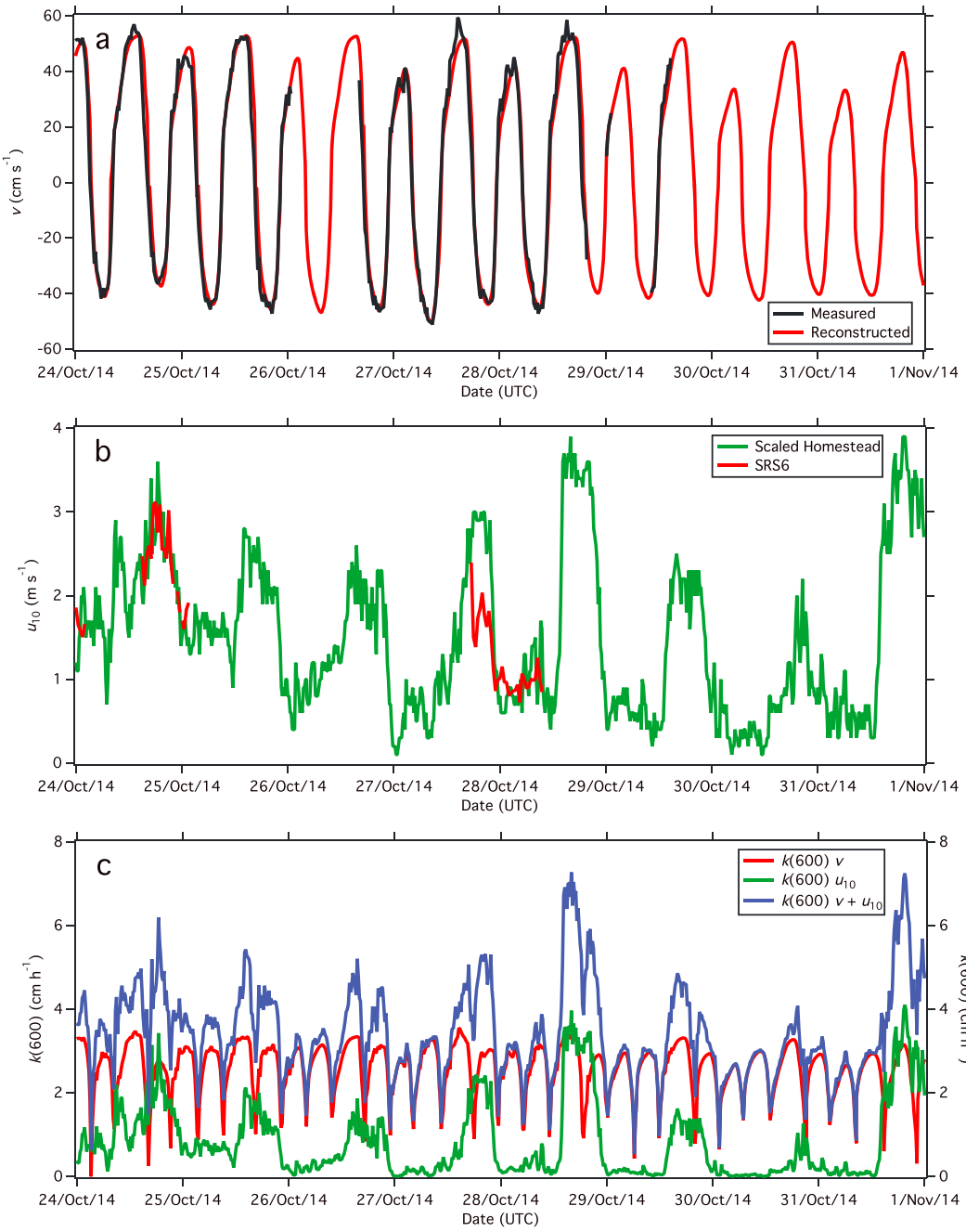

Figure 2. Time series of (a) measured and reconstructed tidal velocities; (b) wind speeds measured in Homestead, scaled to Shark River, and limited wind speeds measured at the CO_2 flux tower at SRS6; (c) gas exchange for Shark River during SharkTREx 3 showing the contribution of current and wind speeds to total gas exchange, as well as the diurnal variability in k(600) due to the diurnal variability in wind speeds.

evening on a gas chromatograph equipped with an electron capture detector using a headspace method [*Wanninkhof et al.*, 1987].

Samples for ^{3}He (approximately 40 mL) were taken in copper tubes mounted in aluminum channels and sealed by stainless steel pinch-off clamps. The samples were stored on the boat until the end of the experiment, when they were shipped back to the laboratory at Lamont-Doherty Earth Observatory for extraction into glass ampules and subsequent analysis on a helium isotope mass spectrometer. For details of the measurement, see *Ludin et al.* [1998].

2.7. $^3He/SF_6$ Technique and Air-Water Gas Exchange

After ^3He and SF_6 are injected at a constant ratio into the water, the change in the $^3He/SF_6$ ratio with time can be used to determine the gas transfer velocity for ^3He ($k_{^3He}$) [*Watson et al.*, 1991; *Wanninkhof et al.*, 1993]:

$$k_{^3He} = -h\frac{d}{dt}\left(\ln\left(^3He_{exc}/SF_6\right)/1 - \left(Sc_{SF_6}/Sc_{^3He}\right)^{-1/2}\right), \quad (1)$$

where h is the mean depth of Shark River at mean tidal height (2.8 m) [*Ho et al.*, 2014], and Sc_{SF_6} (727 to 763) and $Sc_{^3He}$ (108 to 112) are the Schmidt numbers (i.e., kinematic viscosity of water, divided by diffusion coefficient of gas in water) for SF_6 and ^3He, respectively [*Wanninkhof*, 2014]. $k_{^3He}$ is then normalized to Sc of 600, corresponding to Sc of CO_2 at 20°C in freshwater:

$$k(600) = k_{^3He}\left(600/Sc_{^3He}\right)^{-1/2} \quad (2)$$

Multiple stations for $^3He/SF_6$ sampling were occupied over the course of 7 days, and only the samples taken near the peak of the tracer patch (as determined by the SF_6 concentration) are averaged into daily values and used in the analysis. The time evolution of $^3He/SF_6$ can be predicted from an analytical solution to equation (1), starting with an initial $^3He/SF_6$ ratio and a time series of $k(600)$:

$$\left(^3He/SF_6\right)_t = \left(^3He/SF_6\right)_{t-1}\exp\left(-\frac{k_{^3He}\Delta t}{h}\left(1 - \left(Sc_{SF_6}/Sc_{^3He}\right)^{-1/2}\right)\right) \quad (3)$$

The goodness of fit between the measured $^3He/SF_6$ and predicted $^3He/SF_6$ (from equation (3)) will allow parameterizations of $k(600)$ to be evaluated.

2.8. SF_6 Inventory and Residence Time

The daily SF_6 inventory was determined from the underway SF_6 measurements, and the geometry of the river, divided into 100 m longitudinal sections, as follows [*Ho et al.*, 2014]:

$$SF_6 \text{ inventory} = \sum_{i=1}^{n}\left[SF_6\right]_i \times V_i \quad (4)$$

where $[SF_6]_i$ and V_i are the mean SF_6 concentration and volume at midtide in each section i of the river, respectively, and n is the number of sections. The SF_6 concentrations were corrected for tidal movement to slack water before ebb for each day [*Ho et al.*, 2002], before being assigned to a particular section of the river.

The SF_6 inventory decreased each day due to freshwater discharge, tidal flushing (out of the river), and air-water gas exchange. The SF_6 inventory corrected for gas exchange yields the residence time for water in the river and allows different models of residence time to be evaluated. There are a number of models for estimating residence time of water in estuaries [*Sheldon and Alber*, 2006], and the choice of an appropriate one depends on the conditions in the particular estuary (e.g., geometry, circulation, completeness of mixing, and amount of freshwater flow). Here we compute the water residence time, τ, during the three SharkTREx experiments with the freshwater fraction model, chosen because Shark River is influenced to a significant degree by freshwater input from the Everglades marsh upstream:

$$\tau = \frac{V \times \frac{\left(S_{Ocean} - S_{Shark\ River}\right)}{S_{Ocean}}}{Q_{FW}} \quad (5)$$

where V is the volume of Shark River, S_{Ocean} and $S_{Shark\ River}$ are the salinities of the ocean during the incoming tide and the averaged salinity measured in Shark River during each experiment, respectively, and Q_{FW} is the tidally filtered discharge (i.e., net discharge) from the USGS station at Shark River. The salinity of the ocean for each experiment is taken to be the salinity measured from the boat in the Gulf of Mexico.

3. Results and Discussion

3.1. Air-Water Gas Exchange

^3He and SF_6 in the water decreased exponentially over the course of 7 days, due to freshwater input, tidal flushing, and air-water gas exchange. The initial excess ^3He was as high as $24{,}000 \times 10^{-16}$ ccSTP g^{-1} and decreased to 15×10^{-16} ccSTP g^{-1} on the last day of the experiment, while the initial SF_6 concentration

was as high as 48,000 fmol L^{-1} and decreased to 150 fmol L^{-1} on the last day. The background levels of excess ^{3}He and SF_6 during SharkTREx 3 were approximately 2×10^{-16} ccSTP g^{-1} and approximately 1.6 fmol L^{-1}, respectively, so the tracers were still well above background levels on the last day of the experiment.

The change in the ^{3}He/SF_6 ratio is due to gas exchange only (i.e., tidal flushing does not alter the ratio). The mean k(600) for SharkTREx 3, calculated from the decrease in ^{3}He/SF_6 over the course of the experiment using equations (1) and (2), was 3.3 ± 0.2 cm h^{-1}.

The measured decrease in ^{3}He/SF_6 was also modeled using equation (3), with the goodness of fit between model and observations evaluated in terms of relative root-mean-square error (rRMSE):

$$\mathrm{rRMSE} = \sqrt{\frac{\sum_{n=1}^{N} \left[\frac{R^n_{\mathrm{mod}} - R^n_{\mathrm{obs}}}{R^n_{\mathrm{obs}}}\right]^2}{N}} \tag{6}$$

where R^n_{obs} and R^n_{mod} are the observed and modeled ^{3}He/SF_6 ratio, respectively, and N is the number of days during the experiment. It was found that the best fit to the data was given by the combination of a parameterization that takes into account the bottom generated turbulence, based on a modified formulation of *O'Connor and Dobbins* [1958] and the wind speed parameterization of *Ho et al.* [2006], which has been shown to perform well in predicting gas exchange in a large tidal river [*Ho et al.*, 2011a], as well as the open ocean [*Ho et al.*, 2011b]:

$$k(600) = 0.77 v^{0.5} h^{-0.5} + 0.266 u_{10}^2 \tag{7}$$

where 0.77 replaces the original coefficient of 1.539 from *O'Connor and Dobbins* [1958], v is the current velocity (in cm s^{-1}), h is the mean depth of the river (in m), and u_{10} is the wind speed at 10 m height (in m s^{-1}) (Figure 3). Equation (7) is empirical, with the unit conversions embedded in the coefficients. With this formulation, current velocity is the main driver for gas exchange in Shark River and responsible for 79% of the k(600) during SharkTREx 3.

Other wind speed parameterizations derived from the ocean and estuaries were evaluated in combination with the current velocity parameterization proposed above, and in general, the ones derived for the ocean were a better fit to the ^{3}He/SF_6 data than the ones for estuaries (Table 1 and Figure 3). The relationship of *Wanninkhof* [1992] and *Nightingale et al.* [2000] is similar to *Ho et al.* [2006] at the low wind speeds encountered during SharkTREx 3 (0.1 to 3.9 m s^{-1}) and indeed in the range of wind speeds typically measured in Shark River. Hence, these relationships are able to predict k(600) to a reasonable degree during SharkTREx 3. The global parameterizations of *Sweeney et al.* [2007] and *Wanninkhof* [2014], derived from the inventory of bomb radiocarbon in the ocean, are nearly identical to *Ho et al.* [2006] over all wind speeds, so they have equal skills in predicting k(600) during SharkTREx 3. Overall, because the influence of wind on gas exchange in this setting is small, the parameterizations that have nonzero intercepts at $u_{10} = 0$ predict k(600) that were higher than what was observed. This includes the parameterizations of *Borges et al.* [2004], *Jiang et al.* [2008], and *Wanninkhof et al.* [2009]. The parameterization of *Raymond and Cole* [2001] also overpredicts k(600). Table 1 summarizes the mean k(600) calculated from the various parameterizations and the rRMSE for all the parameterizations evaluated.

The mean k(600) found for SharkTREx 3 is less than those previously reported for SharkTREx 1 and 2 (8.3 ± 0.4 and 8.1 ± 0.6 cm h^{-1}, respectively) [*Ho et al.*, 2014] because k(600) determined for SharkTREx 1 and 2 were based on SF_6 inventory, which included the effects of freshwater flow and tidal flushing. By applying the relationship derived above (equation (7)) to current velocities and wind speeds measured during SharkTREx 1 and 2, the revised mean k(600) for SharkTREx 1 and 2 are 3.5 ± 1.0 and 4.2 ± 1.8 cm h^{-1}, respectively. These k(600) estimates give a revised averaged CO_2 fluxes from Shark River during SharkTREx 1 and 2 of 105 ± 9 and 99 ± 4 mmol m^{-2} d^{-1}, respectively, in line with estimates of air-water CO_2 fluxes below the canopy at SRS6 determined by *Troxler et al.* [2015] during the summer of 2011 (88 ± 9 mmol m^{-2} d^{-1}).

3.2. Temporal Variability in Gas Transfer Velocities

From the time series of k(600) (Figure 2c), it can been seen that there is a diurnal signal in k(600), where gas exchange and hence CO_2 flux are higher during the day than at night, due to the strong diurnal signal in u_{10}. Over the course of the experiment, the average daytime k(600) (3.8 ± 1.2 cm h^{-1}) was 36% higher than the

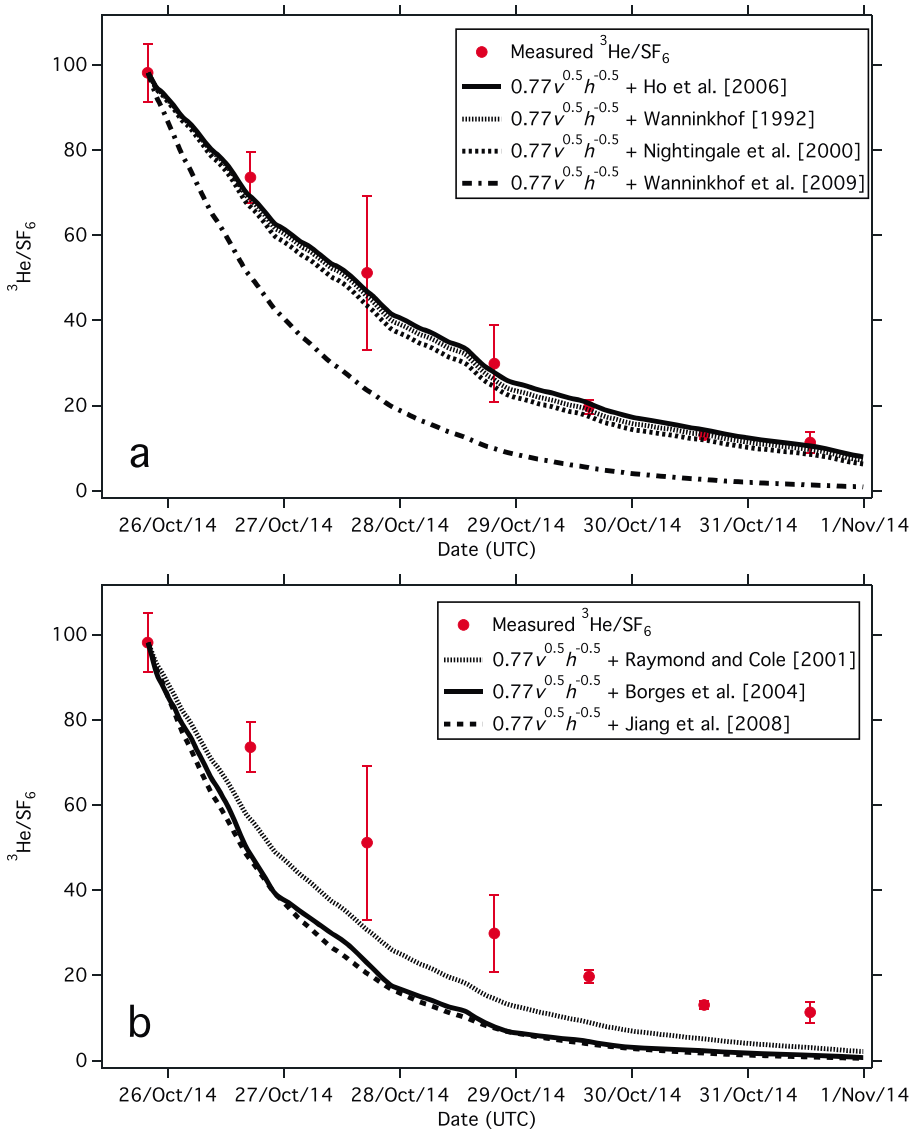

Figure 3. Measured and modeled change in ^{3}He/SF$_6$ ratio over time using parameterizations derived from experiments in (a) the ocean and (b) estuaries. The error bars on the measured ^{3}He/SF$_6$ ratios represent the standard deviations in the individual ^{3}He/SF$_6$ pairs of each day. The parameterizations derived from the ocean, with the exception of *Wanninkhof et al.* [2009], which has a nonzero intercept at $u_{10} = 0$, are significantly better at predicting the decrease in ^{3}He/SF$_6$ than the ones for estuaries.

nighttime $k(600)$ (2.8 ± 0.8 cm h^{-1}). There is an important implication of this finding, as methods to determine gas exchange in wetlands and estuaries are typically only deployed during the day, either because of logistics and safety (e.g., floating chambers) or because the technique precludes them from being used at night (e.g., eddy covariance). If $k(600)$ and CO_2 fluxes are indeed higher during the day, using only data collected during the day might overestimate the overall CO_2 flux from an ecosystem.

3.3. Residence Time

The decrease in SF_6 inventories, corrected for loss due to gas exchange, was used to derive water residence times for Shark River and Tarpon Bay (total water volume: 9.4×10^6 m^3) of 5.8 ± 0.4, 8.1 ± 1.1, and 16.5 ± 2.0 days for SharkTREx 1, 2, and 3, respectively. These residence time values are consistent with the differences in mean (± standard deviation) Q_{FW} (i.e., net discharge) published by the USGS at Shark River of 6.9 ± 5.3, 4.9 ± 15.8, and 2.0 ± 5.0 m^3 s^{-1} for SharkTREx 1, 2, and 3, respectively, where a higher net discharge

Table 1. Gas Transfer Velocities for SharkTREx 3 Determined From Published Parameterizations

Parameterizations	Parameterization[a]	Mean $k(600)$[b]	rRMSE[c]
Modified *O'Connor and Dobbins* [1958]	$k(600) = 0.77v^{0.5}h^{-0.5}$	2.6 ± 0.6	37.6%
	Ocean Parameterizations		
Wanninkhof [1992]	$k(660) = 0.31u_{10}^2$	3.4 ± 1.4	9.5%
Nightingale et al. [2000]	$k(600) = 0.333u_{10} + 0.222u_{10}^2$	3.6 ± 1.3	15.4%
Ho et al. [2006]	$k(600) = 0.266u_{10}^2$	3.3 ± 1.2	7.2%
Wanninkhof et al. [2009]	$k(660) = 3 + 0.1u_{10} + 0.064u_{10}^2 + 0.011u_{10}^3$	6.1 ± 0.8	67.7%
	Estuary Parameterizations		
Raymond and Cole [2001]	$k(600) = 1.58e^{0.3u_{10}}$	5.0 ± 1.1	52.8%
Borges et al. [2004]	$k(600) = 1.0 + 2.58u_{10}$	6.4 ± 2.6	70.7%
Jiang et al. [2008]	$k(600) = 3.99 - 0.43u_{10} + 0.314u_{10}^2$	6.8 ± 1.0	73.9%

[a]The 15 min average wind speeds, 15 min averaged current velocities, and mean depth were used in the calculations. $k(600)$ in cm h^{-1}; u_{10} in m s^{-1}; v in cm s^{-1}; h in m. Some ocean wind speed/gas exchange parameterizations have been expressed as $k(660)$, corresponding to Sc of 660 (close to 666, which is CO_2 in seawater at 20°C). This choice is arbitrary. The conversion from $k(600)$ to $k(660)$ requires a multiplication of 0.953 assuming the dependence of gas exchange on Schmidt number scales to $Sc^{-1/2}$.

[b]Measured $k(600)$ during SharkTREx 3 was 3.3 ± 0.2 cm h^{-1}; the mean $k(600)$ is the sum of the modified *O'Connor and Dobbins* [1958] parameterization and each individual wind speed parameterization; the standard deviation here is the variability in calculated $k(600)$ over SharkTREx 3 and reflects the variability in v and u_{10} rather than uncertainty of each parameterization.

[c]Calculated using equation (6). The relative root-mean-square error gives an indication of the goodness of fit between the modeled and measured decrease in $^3He/SF_6$ during SharkTREx 3. The lower the value, the better the fit.

would lead to a shorter water residence time. Based on these data, an exponential relationship between Q_{FW} and τ can be determined for Shark River ($r^2 = 0.995$):

$$\tau = 3.678 + 26.718e^{-0.367Q_{FW}} \quad (8)$$

This empirical relationship allows a relatively difficult measurement (i.e., residence time of water in Shark River) to be found with easily obtained measurements of Q_{FW}.

Residence times for SharkTREx 1, 2, and 3 were also calculated using the freshwater fraction model (equation (5)). For all three experiments, the model estimated residence times (7.5, 13.0, and 27.5 d for SharkTREx 1, 2, and 3, respectively) that are approximately 14–42% longer than those calculated from SF_6 inventory. This difference could be due to discrepancies in the volume of the river considered in the model, errors in the freshwater discharge estimates, or uncertainties in estimating the freshwater fraction in the river. However, the simplest explanation is that the freshwater fraction model does not explicitly take into account the amount of water (and SF_6) that is lost due to tidal flushing and hence will underestimate the loss rate of water and any substance dissolved in the water.

4. Conclusions

The $^3He/SF_6$ tracer release experiment conducted during SharkTREx 3 has enabled us to derive an integrated parameterization that takes into account the two main sources of turbulence in Shark River, shear generated by tidal currents, and wind stress on the water surface. The results have also allowed us to determine the residence time of water in the river and evaluate the freshwater fraction model.

With this gas exchange parameterization, and continuous measurements of current velocities, wind speeds, and waterside pCO_2, we can determine the temporal variability of CO_2 fluxes from this estuary. In order to know whether the parameterization derived here is applicable to other regions and different estuaries with similar shallow water depths, $^3He/SF_6$ experiments will need to be conducted in those specific settings.

Acknowledgments

We thank the following colleagues for assistance in the field and for participating in SharkTREx 3: Jordan Barr, Carlos Del Castillo, Henrieta Dulai, Gernot Friederich, Jerome Harlay, Damien Maher, Judith Rosentreter, and Dave Stahlke. We thank Mark Zucker at the USGS for providing the current velocity data from the Shark and Harney Rivers and for alerting us to the FAWN wind speed data. The Florida Automated Weather Network (FAWN) run by the Institute of Food and Agricultural Sciences at University of Florida provided the Homestead wind speed data. This experiment would not have been possible without the continued support of Kevin Kotun and Damon Rondeau from the Hydrology Group at Everglades National Park, who provided logistical and material support, including the use of the National Park Service boats. The data used in this manuscript may be obtained by writing to the corresponding author. Funding was provided by the National Aeronautics and Space Administration (NNX14AJ92G) under the Carbon Cycle Science Program.

References

Borges, A. V., J. P. Vanderborght, L. S. Schiettecatte, F. Gazeau, S. Ferron-Smith, B. Delille, and M. Frankignoulle (2004), Variability of the gas transfer velocity of CO_2 in a macrotidal estuary (the Scheldt), *Estuaries*, *27*, 593–603, doi:10.1007/Bf02907647.

Bouillon, S., et al. (2008), Mangrove production and carbon sinks: A revision of global budget estimates, *Global Biogeochem. Cycles*, *22*, GB2013, doi:10.1029/2007GB003052.

Clark, J. F., R. Wanninkhof, P. Schlosser, and H. J. Simpson (1994), Gas exchange in the tidal Hudson River using a dual tracer technique, *Tellus*, *46B*, 274–285.

Clark, J. F., P. Schlosser, H. J. Simpson, M. Stute, R. Wanninkhof, and D. T. Ho (1995), Relationship between gas transfer velocities and wind speeds in the tidal Hudson River determined by the dual tracer technique, in *Air-water Gas Transfer*, edited by B. Jähne and E. Monahan, pp. 785–800, AEON Verlag & Studio, Hanau, Germany.

Ho, D. T., P. Schlosser, and T. Caplow (2002), Determination of longitudinal dispersion coefficient and net advection in the tidal Hudson River with a large-scale, high resolution SF_6 tracer release experiment, *Environ. Sci. Technol.*, *36*, 3234–3241, doi:10.1021/es015814+.

Ho, D. T., C. S. Law, M. J. Smith, P. Schlosser, M. Harvey, and P. Hill (2006), Measurements of air-sea gas exchange at high wind speeds in the Southern Ocean: Implications for global parameterizations, *Geophys. Res. Lett.*, *33*, L16611, doi:10.1029/2006GL026817.

Ho, D. T., P. Schlosser, and P. Orton (2011a), On factors controlling air–water gas exchange in a large tidal river, *Estuar. Coasts*, 1–14, doi:10.1007/s12237-011-9396-4.

Ho, D. T., R. Wanninkhof, P. Schlosser, D. S. Ullman, D. Hebert, and K. F. Sullivan (2011b), Towards a universal relationship between wind speed and gas exchange: Gas transfer velocities measured with $^3He/SF_6$ during the Southern Ocean gas exchange experiment, *J. Geophys. Res.*, *116*, C00F04, doi:10.1029/2010JC006854.

Ho, D. T., S. Ferrón, V. C. Engel, L. G. Larsen, and J. G. Barr (2014), Air-water gas exchange and CO_2 flux in a mangrove-dominated estuary, *Geophys. Res. Lett.*, *41*, 108–113, doi:10.1002/2013GL058785.

Jiang, L. Q., W. J. Cai, and Y. C. Wang (2008), A comparative study of carbon dioxide degassing in river- and marine-dominated estuaries, *Limnol. Oceanogr.*, *53*, 2603–2615, doi:10.4319/lo.2008.53.6.2603.

Levin, A. L., et al. (2001), The function of marine critical transition zones and the importance of sediment biodiversity, *Ecosystems*, *4*, 430–451, doi:10.1007/s10021-001-0021-4.

Ludin, A., R. Weppernig, G. Bönisch, and P. Schlosser (1998), Mass spectrometric measurement of helium isotopes and tritium in water samples, *Tech. Rep. 98-6*, 42 pp., Lamont-Doherty Earth Observatory, Palisades, N. Y.

Maher, D. T., I. R. Santos, L. Golsby-Smith, J. Gleeson, and B. D. Eyre (2013), Groundwater-derived dissolved inorganic and organic carbon exports from a mangrove tidal creek: The missing mangrove carbon sink?, *Limnol. Oceanogr.*, *58*, 475–488, doi:10.4319/lo.2013.58.2.0475.

Nightingale, P. D., G. Malin, C. S. Law, A. J. Watson, P. S. Liss, M. I. Liddicoat, J. Boutin, and R. C. Upstill-Goddard (2000), In situ evaluation of air-sea gas exchange parameterizations using novel conservative and volatile tracers, *Global Biogeochem. Cycles*, *14*, 373–387, doi:10.1029/1999GB900091.

O'Connor, D. J., and W. E. Dobbins (1958), Mechanism of reaeration in natural streams, *Trans. Am. Soc. Civ. Eng.*, *123*, 641–684.

Raymond, P. A., and J. J. Cole (2001), Gas exchange in rivers and estuaries: choosing a gas transfer velocity, *Estuaries*, *24*, 269–274, doi:10.2307/1352954.

Sheldon, J. E., and M. Alber (2006), The calculation of estuarine turnover times using freshwater fraction and tidal prism models: A critical evaluation, *Estuar. Coasts*, *29*, 133–146, doi:10.1007/bf02784705.

Stieglitz, T. C., J. F. Clark, and G. J. Hancock (2013), The mangrove pump: The tidal flushing of animal burrows in a tropical mangrove forest determined from radionuclide budgets, *Geochim. Cosmochim. Acta*, *102*, 12–22, doi:10.1016/j.gca.2012.10.033.

Sweeney, C., E. Gloor, A. R. Jacobson, R. M. Key, G. McKinley, J. L. Sarmiento, and R. Wanninkhof (2007), Constraining global air-sea gas exchange for CO_2 with recent bomb ^{14}C measurements, *Global Biogeochem. Cycles*, *21*, GB2015, doi:10.1029/2006GB002784.

Troxler, T. G., J. G. Barr, J. D. Fuentes, V. Engel, G. Anderson, C. Sanchez, D. Lagomasino, R. Price, and S. E. Davis (2015), Component-specific dynamics of riverine mangrove CO_2 efflux in the Florida coastal Everglades, *Agric. For. Meteorol.*, *213*, 273–282, doi:10.1016/j.agrformet.2014.12.012.

Wanninkhof, R. (1992), Relationship between gas exchange and wind speed over the ocean, *J. Geophys. Res.*, *97*, 7373–7381, doi:10.1029/92JC00188.

Wanninkhof, R. (2014), Relationship between wind speed and gas exchange over the ocean revisited, *Limnol. Oceanogr. Methods*, *12*, 351–362, doi:10.4319/lom.2014.12.351.

Wanninkhof, R., J. R. Ledwell, W. S. Broecker, and M. Hamilton (1987), Gas exchange on Mono Lake and Crowley Lake, California, *J. Geophys. Res.*, *92*, 14,567–14,580, doi:10.1029/JC092iC13p14567.

Wanninkhof, R., W. Asher, R. Weppernig, H. Chen, P. Schlosser, C. Langdon, and R. Sambrotto (1993), Gas transfer experiment on Georges Bank using two volatile deliberate tracers, *J. Geophys. Res.*, *98*, 20,237–20,248, doi:10.1029/93JC01844.

Wanninkhof, R., W. E. Asher, D. T. Ho, C. Sweeney, and W. R. McGillis (2009), Advances in quantifying air-sea gas exchange and environmental forcing, *Annu. Rev. Mar. Sci.*, *1*, 213–244, doi:10.1146/annurev.marine.010908.163742.

Watson, A. J., R. C. Upstill-Goddard, and P. S. Liss (1991), Air-sea gas exchange in rough and stormy seas measured by a dual tracer technique, *Nature*, *349*, 145–147, doi:10.1038/349145a0.